

The Influence of the Ionospheric Scintillation on the GMS Communication Link

Tetsuro Fukui* and Masatoshi Matsuo*

Abstract

The influence of the ionospheric scintillation on the satellite communication link becomes a remarkable problem, because the satellite communication is very active. This report will review the researches and the observations of the GMS communication link will be described. As for the GMS link, the condition of the link has been continuously monitored by recording the receiving signal level of the telemetry channel, these data will be classified and the characteristics of the scintillation will be shown. The data of a big scintillation, which is classified as a largest scale and was observed on 15 February 1978, will also be described.

1. Introduction

With the development of the satellite communications, it has been understood that the ionospheric scintillations have a great influence on the communication link between the satellite and the earth. Formerly the radio waves of frequency bands (GHz band) used for Geostationary Meteorological Satellite (GMS) were considered to be transparent in the ionosphere and in the troposphere, it has been observed since the beginning of the satellite communications that the radio waves of GHz band were suffered irregular fluctuations or scintillations of amplitude, phase and angle after penetrating the ionosphere.

Since the scintillation of the geostationary satellite radio waves began to be continuously observed, the general idea the irregularity of the electron density in the ionosphere has been better understood. As for the severe scintillations, which are occasionally observed during geomagnetic storms, however, data provided

on this subject are scarce and don't allow satisfactory clarification to be made on its characteristics and relationship with other geophysical phenomena.

This report will briefly review the mechanism of scintillation and describe about the scintillation data observed on the GMS communication link.

2. The mechanism of the scintillation

2.1 Solar activity and the ionosphere

The ionospheric scintillation has been observed at frequencies ranging from 10 MHz to 10 GHz. This phenomenon is now considered to be caused by the diffusion of radio waves which is a result of the ionospheric electron density irregularity. As for the effect of the solar activity on the earth's magnetic field, there have been many kinds of researches and observations showing that the ionospheric turbulences cause the interference of the short wave communications, cause the aurora in the polar region.

Recently the relation between the solar activity and the earth's magnetic field is becoming clearer, because it has become possible to carry

* Meteorological Satellite Center.

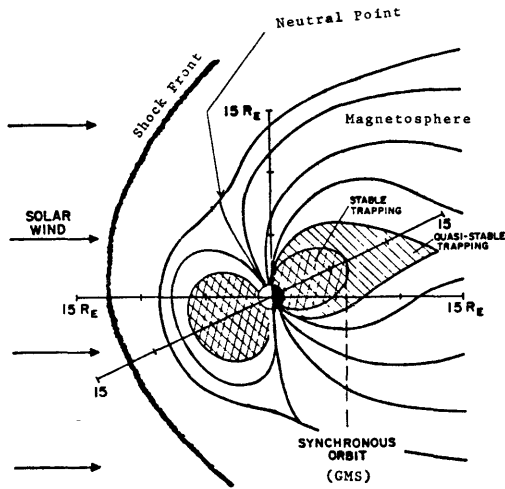


Fig. 1 The relative location of the Earth's magnetic field and the Plasma Regions Dominating Rynchronous orbit.

various observation methods into the space using satellites and the space to earth communications have become active. As a result of these observations, the mechanism of the ionospheric disturbance is explained as follows.

Without the influence of the outer space, the geomagnetic field is the dipole field, however, actual geomagnetic field is distorted by the solar wind (plasma) as shown by Fig. 1.

The radiation from the sun contains sufficient energy at short wavelength to cause appreciable photo-ionization of the earth's atmosphere at

high latitudes. Thus the sun's radiation gives rise in the upper atmosphere to a partially ionized region known as the ionosphere. The recombination of the ions and electrons which are produced in this manner proceeds slowly enough at the low gas densities involved so that fairly high concentrations of electrons persist even throughout the night. During the daytime, several distinct ionospheric "layers" or "regions" are recognized.

If the solar activity altered, the ionosphere would be suffered such influences as shown by the Table 1.

The magnetic storms and the ionospheric scintillations which are dealt with in this report have relation with the high speed plasma which is radiated from the flare area in the sun. It is known that the plasma, of which density is several particle/cm³ and the speed is about 400 km/sec, is continuously radiated from the sun and is called as the solar wind. If the high speed plasma, which was accelerated up to the speed of 500-900 km/sec in the flare region, came accompanied by the continuously blowing solar wind, it was disseminated through the interplanetary space causing the shock wave then it reached at the front of the earth's magnetic field two or three day after the solar flare. The magnetic storm might be occurred

Table 1 The kinds of the ionospheric turburence.

Name of Disturbance	Location	Time Log (after the flare)	Duration	Caue
Sudden Ionospheric Disturbance (SID)	Day-Time	8 minutes	0.5-3 hours	X-ray
Polar Cap Disturbance (PCD)	Polar Region	1-2 hours	several day	High speed Proton and Electron
Ionospheric Storm	All over the Earth	2-3 day	2-3 day	High speed Plasma (Flare)
Regressive Ionospheric Disturbance	All over the Earth	3-4 day after crossing the solar meridian of corona hole. 27 days cycle	several days	High speed Plasma (Corona hole)

at this time. It is reported in recent research that the arrival of the high speed plasma doesn't always cause the magnetic storm but the southward component must exist within the magnetic field of the high speed plasma.

2.2 The aspect of the scintillations

Scintillations as discussed by this report are variations of amplitude, phase, polarization and angle-of-arrival produced when radio waves pass through electron density irregularities in the ionosphere. The scintillations can become quite severe and may represent a practical limitation for some communication systems. Data showing scintillation have been observed on frequencies from 10 MHz through the UHF band to 11 GHz, the bulk of data being observations of amplitude scintillation in the VHF band.

The fading period of scintillation varies over quite a large range and can be as long as several minutes (Koster, 1966). The fading period depends both upon the apparent motion of the irregularities relative to the ray path, and in the case of a strong scintillation, on its severity. For strong scintillation the fading period is shorter than for weak scintillation with the same relative velocity.

The ionospheric electron density irregularity, which causes the scintillation, is distributed over various altitude. The effective irregularities for scintillation are in the F region, which is several hundred km high, and in the sporadic E layer, which is about 100 km high.

Sometimes the F region shows a diffuse character which is attributed to clouds of electrons having concentrations different from the ambient surroundings. This condition is called "spread F", and it occurs mainly at night (Write et al., 1956). Since the dielectric constant of the ionosphere varies with the electron concentration, these inhomogeneities cause scin-

tillation of signals from radio stars of other radio sources beyond the ionosphere. The phenomena of spread F occur more often at high latitudes during periods of high sunspot activity, show a minimum at all times near 35-deg geomagnetic latitude, and occur more often at low latitudes during periods of low sunspot activity.

The spread F, which has relation to the scintillation observed in Japan, is thought as the geomagnetic equator type. This type of irregularity is assumed to have relation to the vertical motion of the ionospheric plasma, which is caused by interaction between the electric field of the ionosphere and the earth's magnetic field.

One model that is gaining acceptance states that the collision-dominated Rayleigh-Taylor instability sets up primary irregularities. Essentially in the first phase after the post sunset rise of the F layer, the density contours are distorted by irregular vertical motions and the growth of the larger scale irregularities starts. The irregularities less than 1 km grow on the primary irregularities possibly by the drift wave instability mechanism (B. B. Balsley et al. 1972). The type of spread F appears to vary during the night. The post sunset start of spread F is predominantly of the range spread type (S. K. Chatterjee et al. 1974). After midnight and before sunrise the frequency spread type dominates.

2.3 Frequency dependence of scintillation

It is known that the influence of the scintillation is different in proportion to the frequency, Rufenach reviewed the frequency-dependence observations and found that some of the measurements were not consistent with the weak-scintillation model. Using a spectral index η to describe the wave-length dependence λ^η , he found η values of both 1.5 and 2.

2.4 Geometrical characteristics

The intensity at which scintillations are observed depends upon the position of the observer relative to the irregularities in the ionosphere that cause the scintillation. Such as zenith angle of the propagation path at the ionospheric layer, propagation angle relative to the earth's magnetic field, and the distance from the irregularity region to the source and to the observed (near the irregularities, only phase fluctuations are developed) are related to the observed intensity of the scintillations.

Equatorial ionospheric scintillation is primarily a nighttime phenomenon, with more severe fluctuations occurring pre-midnight. Scintillation activity peaks near the equinoxes in the South American and African sectors, but the seasonal variation at other longitudes is not yet certain. Equatorial scintillation, the boundary of which lies between 20° and 30° geomagnetic latitude (Taur, 1973), exhibits a long-term positive correlation with sunspot number (Taur, 1974). Fading to 6 GHz has been noted on long term observations in the equatorial

Table 2 Solar-geophysical and temporal dependence of ionospheric scintillation.

Parameter	Equatorial	Mid-latitude	High-latitude
Activity level	Exhibits greatest extremes	Generally very quiet to moderately active	Generally moderately active to very active
Diurnal	Maximum-night-time Minimum-day-time	Maximum-night-time Sporadic-day-time	Maximum-night-time Minimum-day-time
Seasonal	Longitudinal dependent Peaks in equinoxes Accra, Ghana Maximum-November and March Minimum-solstices Huancayo, Peru Maximum-October-through March Minimum-May through July Nwajalein Islands Maximum-May Minimum-November and December	Maximum-spring Minimum-winter Tokyo, Japan Maximum-summer Minimum-winter	Maximum-summer Minimum-winter
Solar cycle	Occurrence increases with sunspot number	Insufficient data	Occurrence increases with sunspot number
Magnetic activity	Longitudinal dependent Accra, Ghana Occurrence decreases with K_p Huancayo, Peru March equinox- Occurrence decreases with K_p June solstice- Occurrence increases with K_p September equinox, 0000-0400 h (local time) Occurrence increases with K_p	Independent of K_p	Occurrence increases with K_p

region (Skinner et al., 1971).

The equatorial latitudes show greater depth of scintillation than the auroral regions. The occurrence of scintillation in the equatorial region appears to be greatest at the equinoxes, and is positively correlated with solar flux and shows a tendency to be inversely correlated with magnetic activity (Mullen, 1973).

At mid-latitudes there is a variation with time of day and with latitude as well as season and epoch of the solar cycle. The diurnal variation of mid-latitude scintillation shows a well-established maximum nearmidnight which correlates with the occurrence of inospheric spread F. A second maximum around midday has also been found in some sets of observations. This is most pronounced in summer, and there is evidence for its association with sporadic E (AAarons and Whitney, 1968). Data collected during quiet and disturbed magnetic conditions indicate little correlation between mid-latitude scintillation and magnetic activity.

High latitude scintillation shows a sharp equatorward boundary, the position of which depends on time of day and magnetic activity. Poleward of the boundary, scintillation maximize over aurora.

Compared to mid-latitude levels, scintillation of radio signals increases considerably when the ray path traverses the high latitude region. The increase starts with the boundary of low level irregularities located at night in the same region as the ionospheric trough. Scintillations maximize above the aurora. At polar latitudes, scintillation level is high but somewhat lower than at auroral latitudes. During periods of magnetic activity, scintillation levels increase dramatically with local excursions of the magnetic field. Table 2 shows the above mentioned scintillations.

Fig. 2 (Aarons et al., 1971) is a generalized map of the nighttime hemisphere showing de-

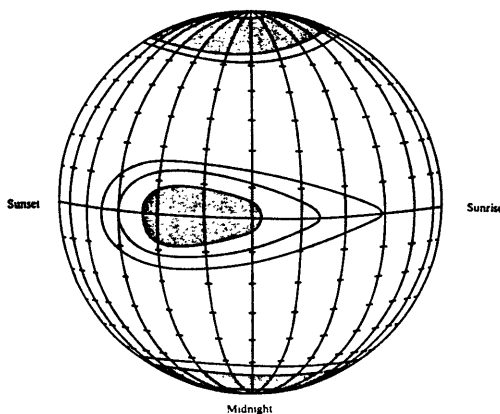


Fig. 2 Night-time picture of scintillation occurrence. The density of matching is proportional to the occurrence of deep facting.

pth of fluctuation as a function of local meridian time for a year of relatively high solar activity. The depth of fluctuation is proportional to the shading density of the figure. The map of Fig. 2 was derived primarily from measurements made at 136 MHz.

2.5 The environment of the geostationary satellite

The synchronous orbit environment (6.62 earth radii from the center of the earth) is unique in the variability of the plasma and field characteristics encountered. Interior to synchronous orbit, the earth's magnetic field is sufficiently strong that it effectively dominates charged particle motion. Near synchronous orbit the collective kinetic energy of the ambient particles is sufficient to alter the constraining magnetic field and cause large variations in plasma conditions on a small time scale. The occurrence of rapid charges on plasma parameters associated with the injection of high temperature plasma into the synchronous orbit regime is the most important factor in spacecraft charging. Fig. 1 depicts the location of the synchronous orbit environment. (H. B. Garret et al., 1977). The change of the

spacecraft charging, which in equivalent of the sheath impedance changing of the spacecraft, is assumed to cause the variation of the spacecraft's output power. Fig. 1 shows that the geostationary satellite is situated in the boundary region where the solar particles, which are trapped by the earth's magnetic field, are in the stable state or in the quasi-stable state according to the solar activities. Consequently, this changing of the state of the solar particles cause the above mentioned phenomena.

3. Scintillations on the GMS communication link

Since May 1977, the scintillations have been observed by the geostationary satellite such as Engineering Test Satellite-2 (ETS-2), GMS, Communication Satellite (CS) and so on. Although the scintillation data are scarce and are not satisfactory analyzed, the data obtained in Japan are valuable to study the mid-latitude scintillations. The GMS was launched July

1977 and the receiving signal level of Telemetry Channel had been continuously recorded. Various scintillations which are recognized in this data will be described here. Some part of these observed data were reported to the Comite Consultatif International des Radio Communications (CCIR) and the Coordination on Geostationary Meteorological Satellite (CGMS).

3.1 Ground instrumentation and data handling

The frequency allocation of the GMS communication link is shown by Fig. 3 and the scintillations are observed by the signal of Telemetry channel. The Telemetry signal is being used for the pilot signal of the tracking receiver, accordingly the signal level of the receiver AGC is continuously recorded. The overall system of the Command and Data Acquisition Station (CDAS) is shown by Fig. 4 and the functional block diagram of the tracking receiver is shown by Fig. 5.

The parameters of the telemetry channel and

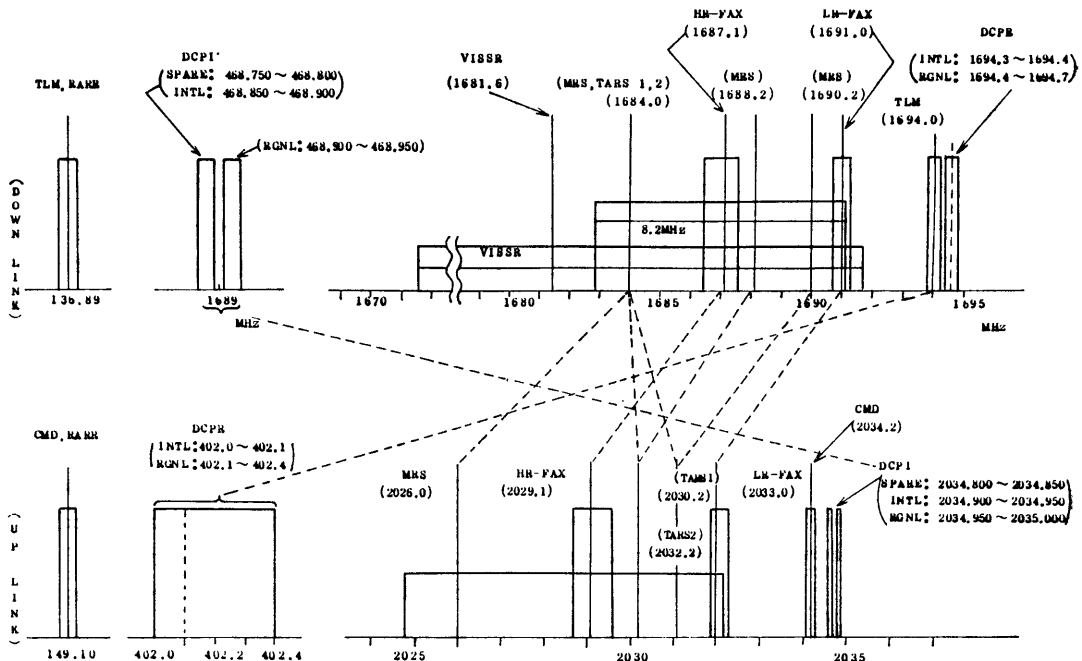


Fig. 3 Frequency allocation of the GMS up link and down link.

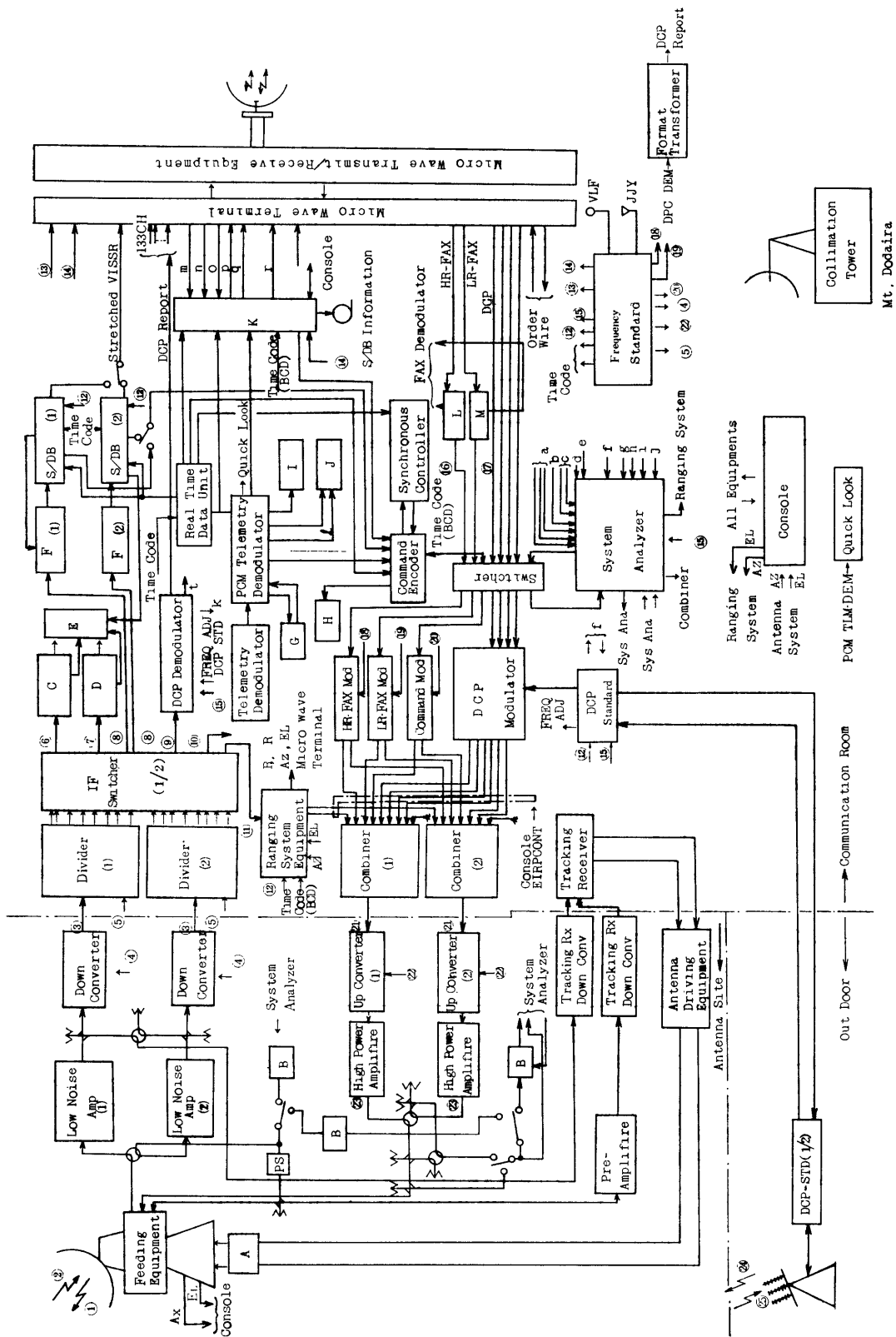


Fig. 4 (The caption is given on the next page.)

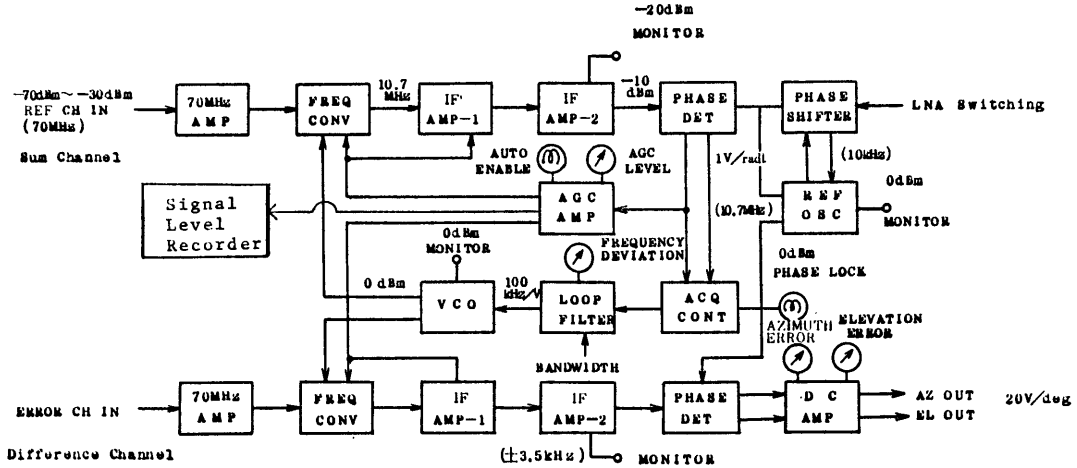


Fig. 5 Functional Block Diagram of the tracking receiver.

the characteristics of the 18 mφ Antenna are shown by Table 3 and Table 4, respectively. The nominal receiving level of the telemetry channel is shown by Fig. 6. In this Fig. 6, S1 Mode means the observation using the Visible and Infrared Spin Scan Radiometer (VISSR), S2 MODE means the measurement of range and range rate, S3 MODE means the dissemination of the High Resolution Facsimile, S4 MODE means the dissemination of the Low Resolution Facsimile. The signal level changes because the spacecraft's output powers are not the same in each mode. There is the fluctuation of the signal level (≈ 1.5 db), which is the resultant of the spacecraft spin (spin ripple).

3.2 The result of the observation

The seasonal variations of scintillation occurrence of GMS communication link are shown by Fig. 7-a and Fig. 7-b. The scintillations are most active in the summer season (May-August), and quiet during the winter season. The distribution of the occurrence of the scintillations, of which signal level fluctuation exceed 0.5 db peak to peak, is shown by Fig. 8-a and Fig. 8-b. Fig. 9 shows the various satellite's anomalies, this data shows the same tendency as of the GMS. The duration and the maximum amplitude of the scintillation in 1978 are shown by Fig. 10-Fig. 13.

Fig. 4 CDAS System Block Diagram

- ① 2,024~2,036 MHz
- ② 1,671~1,695 MHz
- ③ 70 MHz 1F
- ④ 1 611.6/36 MHz
- ⑤ 8.4 MHz STD
- ⑥ 67.1 MHz
- ⑦ 71 MHz
- ⑧ 70 MHz
- ⑨ 74.5 MHz
- ⑩ 74 MHz
- ⑪ 64, 68.2 MHz
- ⑫ 1 MHz STD
- ⑬ 1 kHz STD
- ⑭ 1 Hz STD
- ⑮ 5 MHz STD
- ⑯ 99 kHz
- ⑰ 2.4 kHz
- ⑱ 67.1 MHz STD
- ⑲ 71.0 MHz STD
- ⑳ 7.22 MHz STD
- ㉑ 70 MHz 1F
- ㉒ 1,962/36 MHz
- ㉓ 2 GHz 2 kW
- ㉔ 402.2 MHz
- ㉕ 468.875 MHz
- ㉖ 468.924 MHz

- a. DCP Mod. b. Command. c. HR/LR FAX Mod. d. IF Switcher e. Ranging f. DCP Demodulator g. Telemetry Demodulator h. HR FAX DEM. i. LR FAX DEM. j. Ranging System k. System Analyzer l. Slow Code m. Command n. S/DB Information o. DPC Information p. PCM TLM q. Real Time r. CDAS Information s. Ranging Data t. Format Transformer A. Drive Motor B. System Analyzer C. HR-FAX Demodulator D. LR-FAX Demodulator E. Image Monitor F. 4φ DEMOD/DEMUX G. Mag Tape Recorder H. Command Recorder I. Digital Printer J. Pen Recorder K. Communication Control Unit L. HR-FAX Sub Carr. Mod. M. LR-FAX Sub Carr. Mod.

Table 3 The characteristics of GMS Telemetry channel.

Satellite link	GMS-CDAS
Frequency (MHz)	1694.0
Type of Moduration	PCM-PSK FM-PM (AM-PM)
E. I. R. P. (dbm)	42.9
Tx Off-beam center (degree)	6.5
Tx Off-beam center Loss (db)	-1.4
Free Space Loss (db)	-188.4
Rx Off-beam center (degree)	0.1
Rx Off-beam center Loss (db)	-0.6
Rx Input power Level (dbm)	-147.5
Rx System Noise temp. G/T (db/°K)	29.3
Rx C/T (db/°K·Hz)	-118.2
Boltsman's Constant (dbm/°K)	-198.6
C/No (db/Hz)	80.4
Total C/No (db/Hz)	80.4
Required C/No (db/Hz)	70.2
Margin (db)	10.2
C/N (db)	

Table 4 The characteristics of 18 mφ Antenna.

Receiving	
Frequency	1666 MHz~1698 MHz
Antenna Gain	More than 47.5 db
Noise temperature	Less than 35°K
VSWR	Less than 1.3
Side lobe Level	Less than -14 db
Beam Width	0.66 deg

3.3 The scintillation on 15 Fedurary 1978

A typical scintillation was encountered at 20:00 UT, Feburary 1978. The amplitude of fluctuations exceeded 15 db and the function of the antenna auto-track failed. The occurrence time and the period of duration are shown in Fig. 14 together with the observation data of ETS-2 and CS. Fig. 15 shows the

relation between the propagation path and the geographic latitude of three geostationary satellites and observation stations. Considering the beginning time of scintillations and the geometrical propagation path, these phenomena seemed to move west to east at the altitude of about 600 km.

The Space Environment Monitor (SEM) data of GMS and SMS-2 are shown by Fig. 16-Fig. 19. These data indicate that particles rediated from the solar flare, which occurred at 15°N, 20°W on the sun at 13:30 UT, 13 Feburary 1978, reached the geostationary satellites 2 or 3 hours after. Observation data of Kakioka Magnetic Observatory in Japan show that a magnetic storm occurred about 21:45 UT 14 Feburary, 1978 and this time is much the same as the rising point of P2 in Fig. 17. Fig. 20 shows the relation between radio frequencies and the amplitude of scintillations, the data of which were obtained from Radio Research Laboratory in Japan. These data indicate that the scintillation on 15 Feburary, 1978 was a big one and the frequency range affected by it reached about 11 GHz band. This event may be ranked as the most active scintillation, and it was typically shown that the solar particles radiated from the solar flare had influence of the earth's magnetic field.

4. Conclusion

As the scintillation data of mid latitude are scarce, which were described above, the relation between the scintillations and solar activity or other ionospheric phenomena is not yet become clear. It will be very effective to analize such scintillation data obtained by geostationary satellite as the seasonal variation data, the diurnal variation data and so on. The GMS link have experienced many scintillations but such scintillation was very few that the communication link was disturbed, for instance the

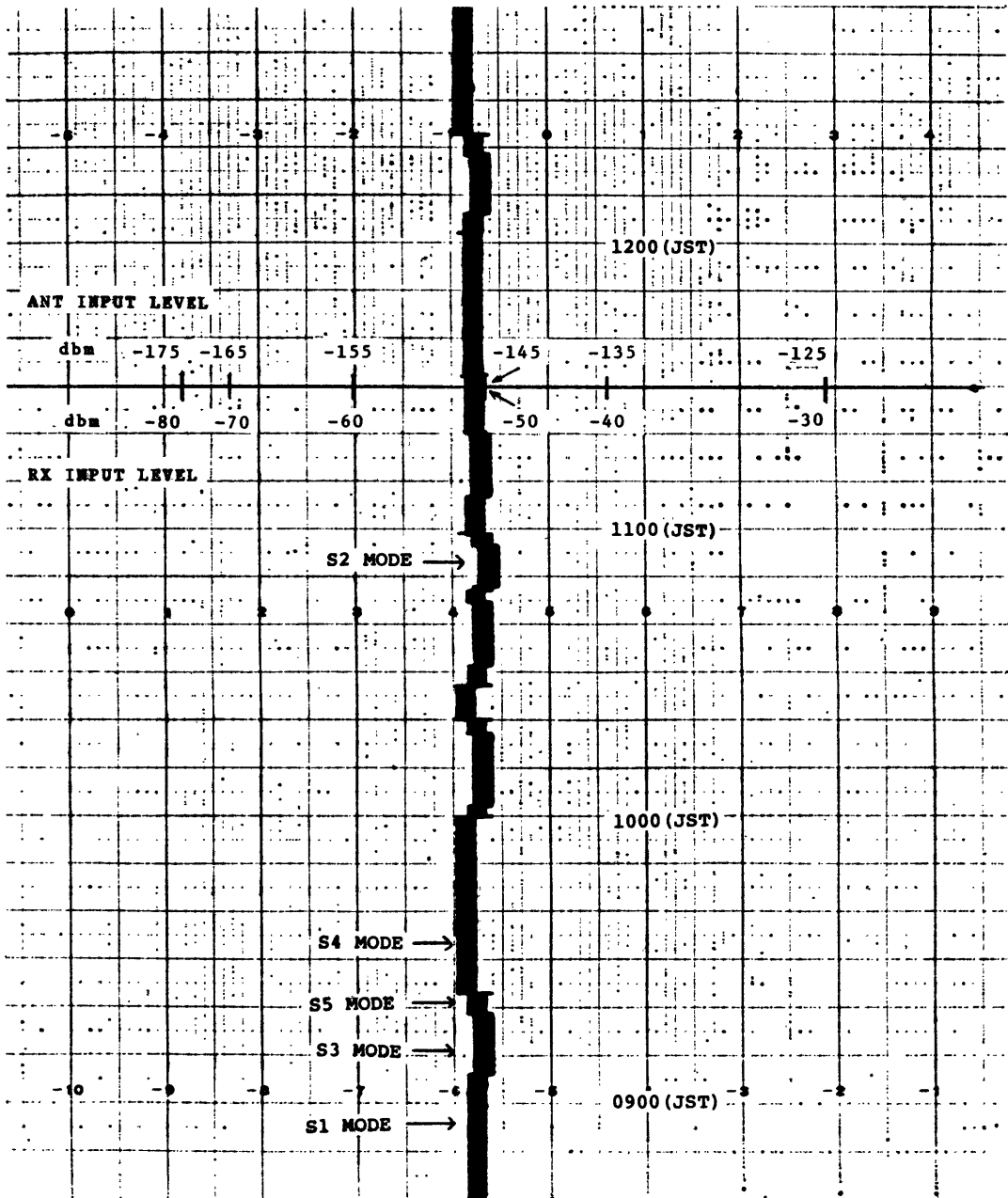


Fig. 6 Record chart of the telemetry signal.

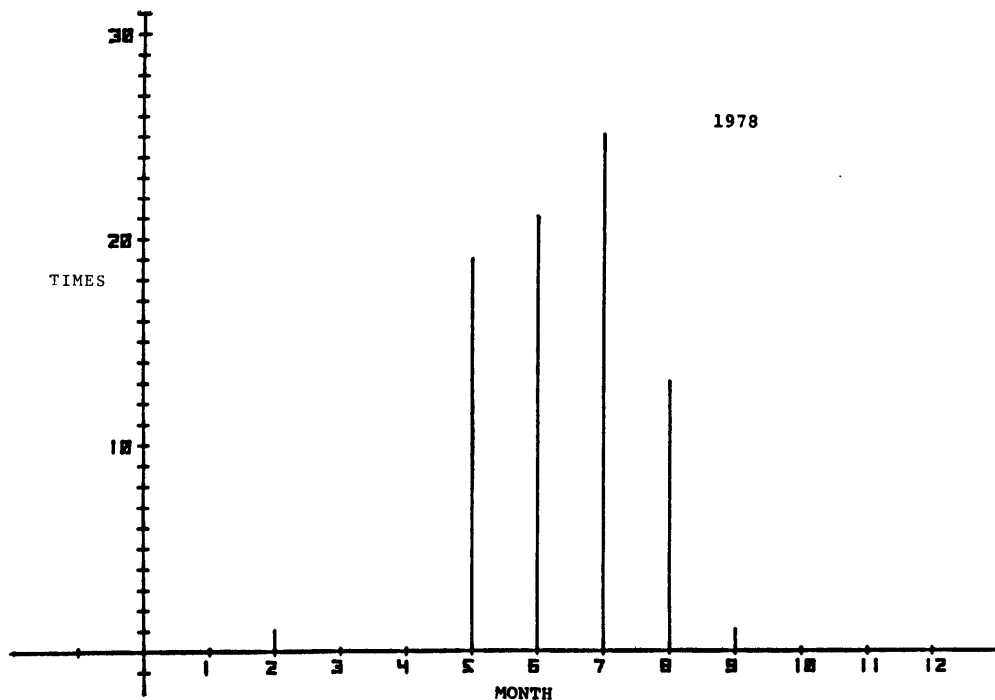


Fig. 7-a Seasonal variations of the scintillations of GMS link.

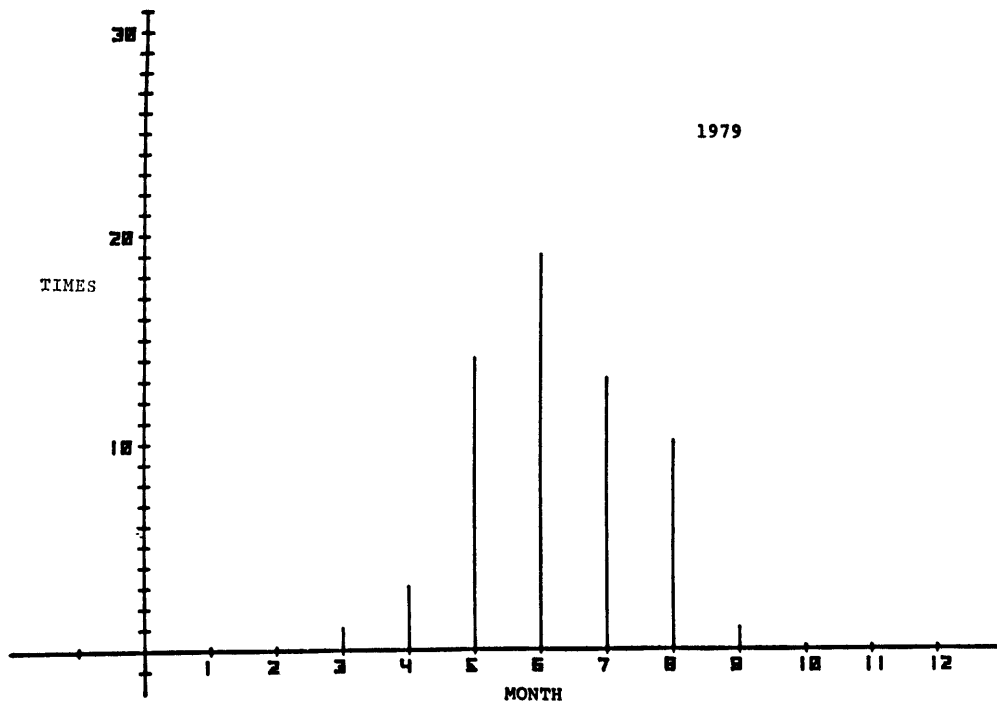


Fig. 7-b Seasonal variations of the scintillations of GMS link.

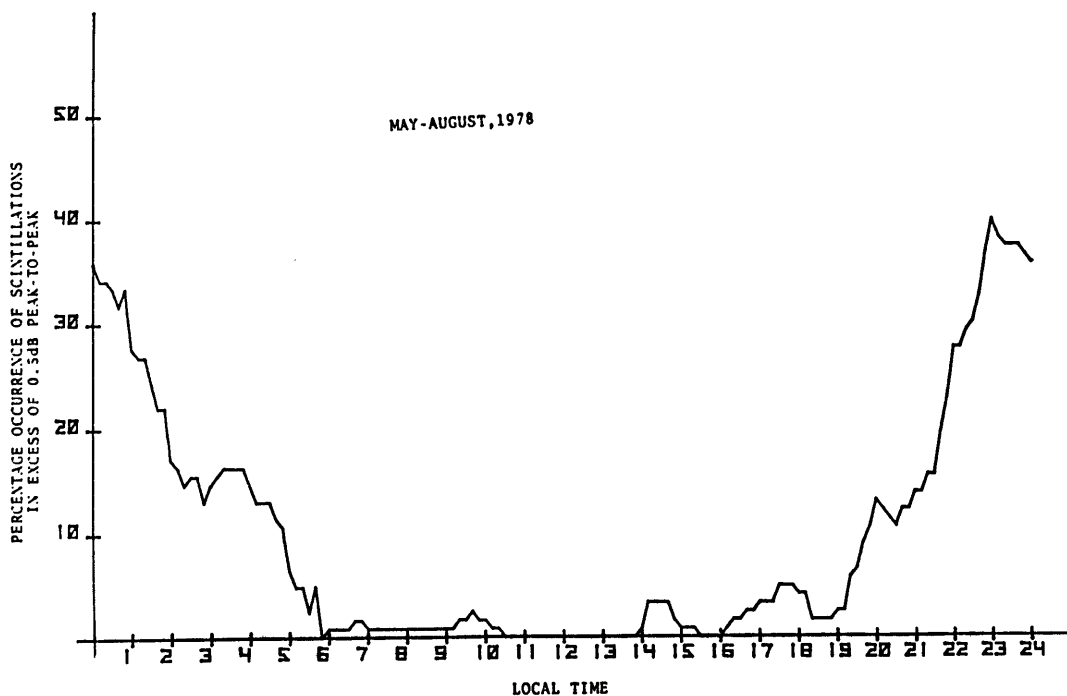


Fig. 8-a Diurnal variation of scintillation occurrence of GMS link.

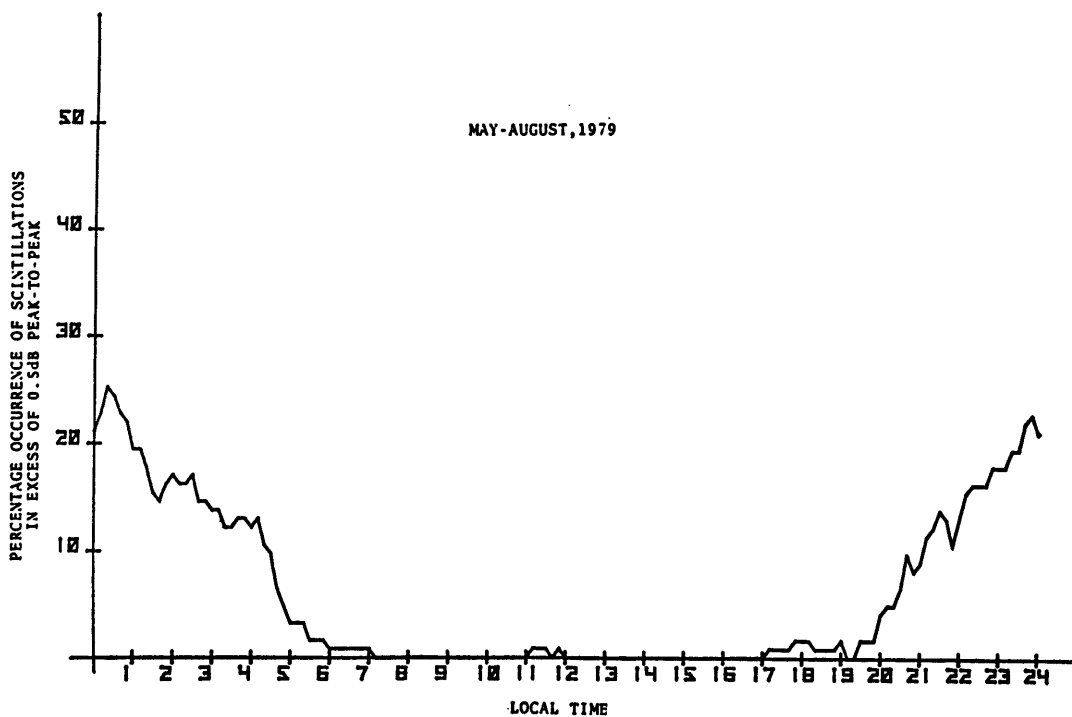


Fig. 8-b Diurnal variation of scintillation occurrence of GMS link.

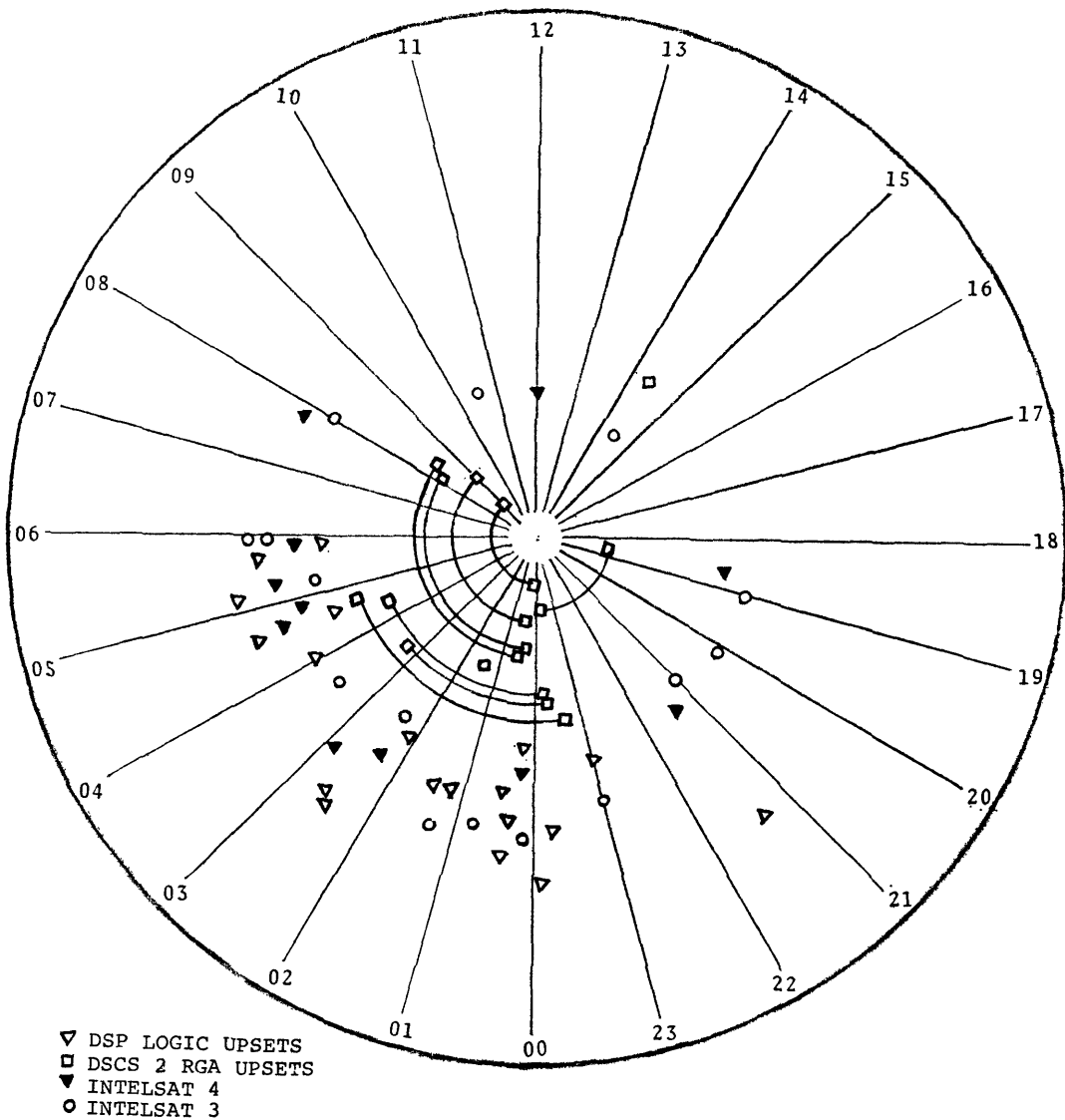


Fig. 9 Local time plot of various satellite disruptions and anomalies. The radial variations are not real but merely for graphical representation.

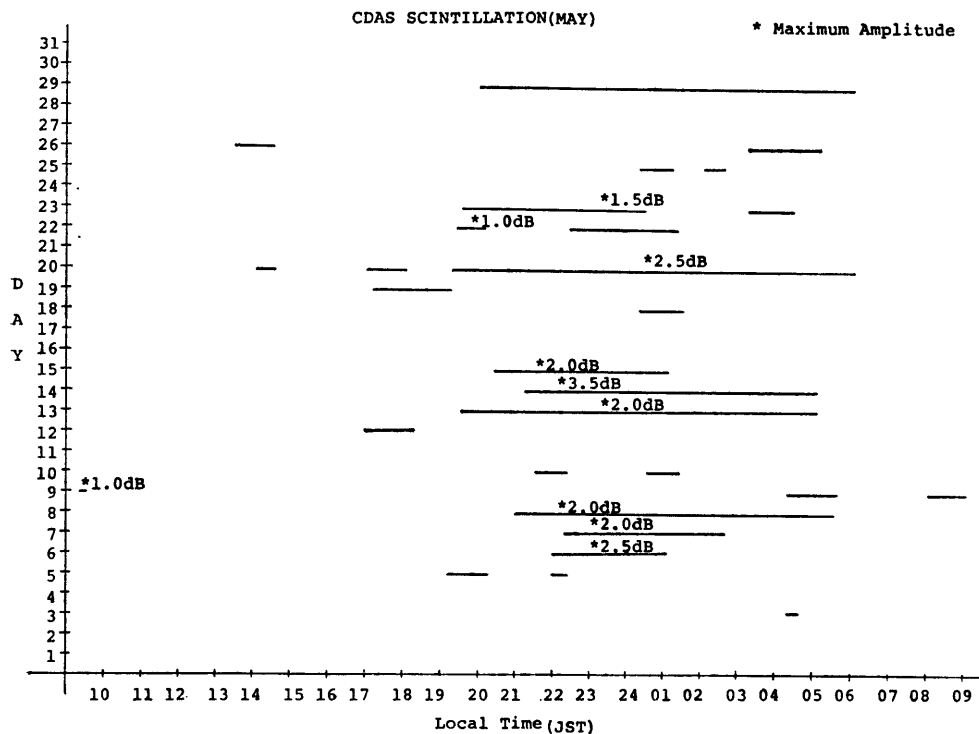


Fig. 10 Duration of scintillation in 1978.

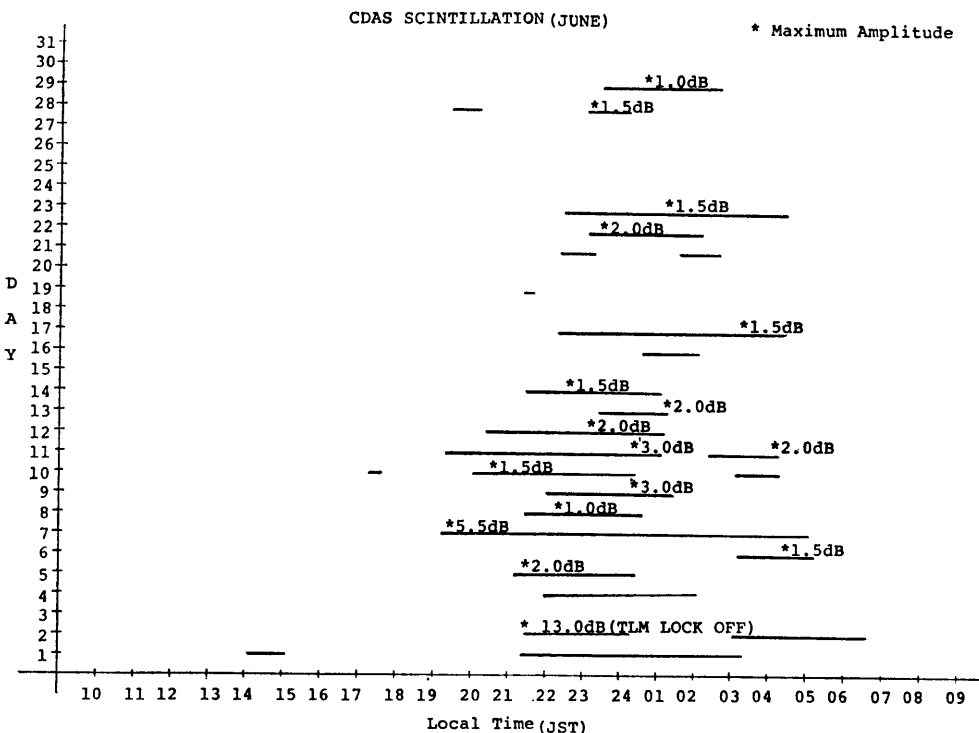


Fig. 11 Duration of scintillation in 1978.

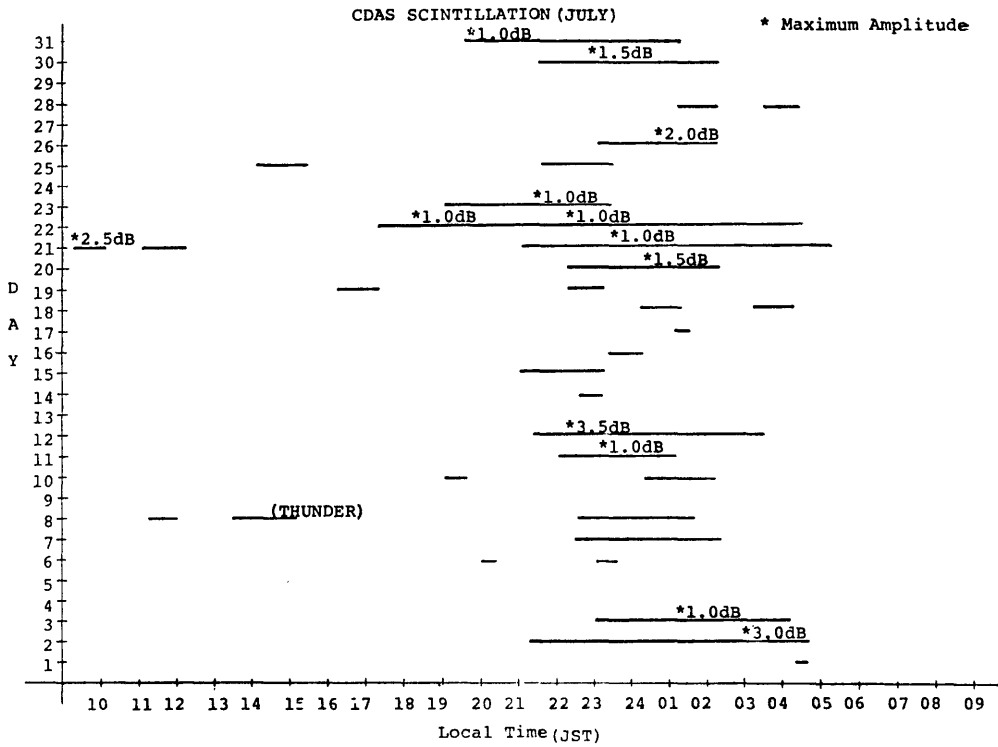


Fig. 12 Duration of scintillation in 1978.

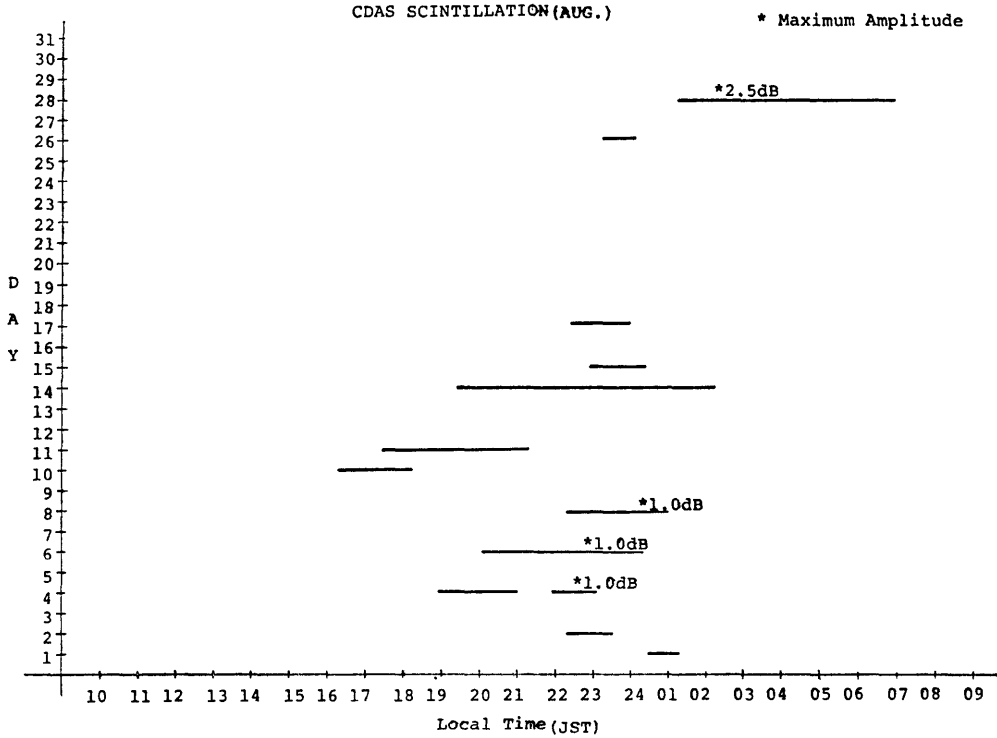


Fig. 13 Duration of scintillation in 1978.

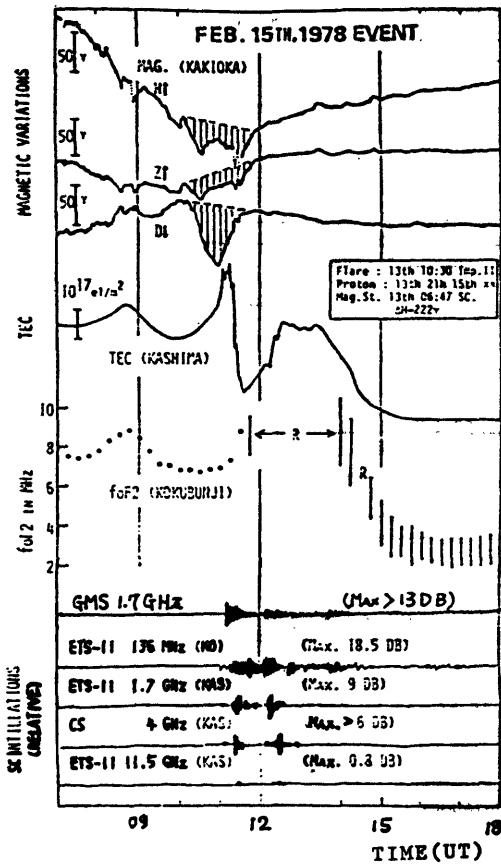


Fig. 14 The aspects of geomagnetic field, ionosphere and scintillation of satellite signal on 15 February, 1978. (K. Shinno: Radio Regulation Laboratory of Japan)

function of the antenna auto track was failed or other GMS mission was stopped. This is because the GMS communication link is designed to have enough margin and the frequency band used is suffered from relatively few scintillation.

Concerning the Medium Scale Data Utilization Station (MDUS), the Small Scale Data Utilization Station (SDUS) and the Data Collection Platform (DCP), the margin of the communication link is not so large as the GMS-CDAS link. It can be assumed that these links may be more affected by scintillation, however, there is no observation data.

It is very difficult to predict the occurrence of scintillation, at present. In case of 15 Febu-

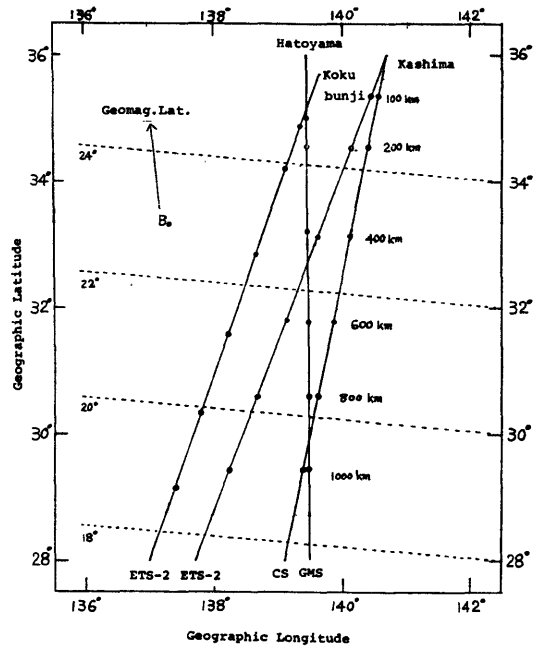


Fig. 15 The propagation path and the geographic latitude of three geostationary satellites and observation stations. (M. Fujita et al., 1978: Radio Regulation Laboratory of Japan)

ruary Event, the SEM data, the magnetic storm data and the scintillation data indicate a good correlation, but such a case is very few. Informations about the ionospheric anomalies are now being exchanged between JMA and the Radio Regulation Laboratory. Even if the value of the SEM was different from normal value and the radio warning was announced, the scintillation of 1.7 GHz band was not always observed. It is necessary to accumulate the various kinds of data for analyzing the phenomena.

In preparing this presentation, the authors wish to thank Dr. Shinno, who is the Chief of the First Special Study Room, for his helpful advice and offer of data, and also other members of Radio Regulation Laboratory. Thanks are also due to Mr. H. Konishi who is the member of CDAS and assisted to adjust the scintillation data.

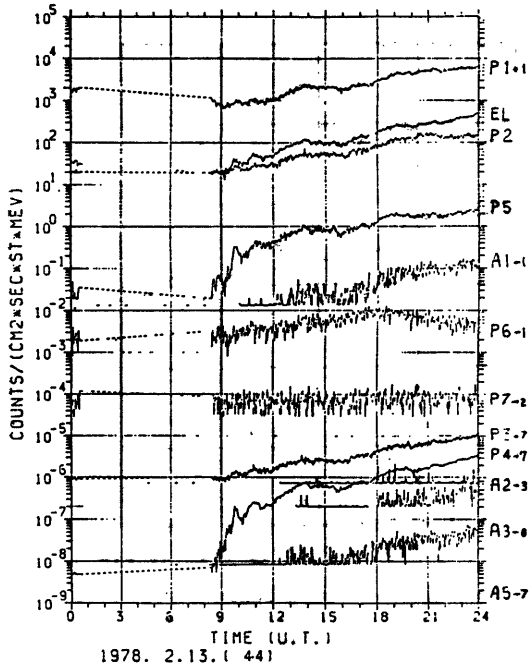


Fig. 16 The two minutes average of the space environmental monitor which is installed on GMS.

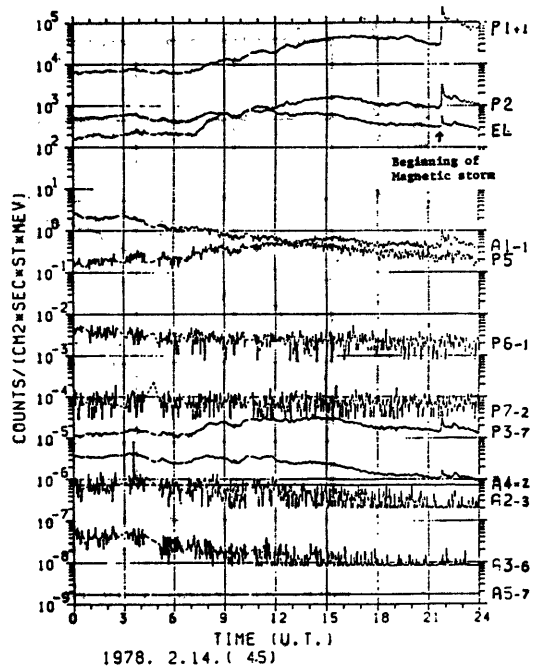


Fig. 17 The two minutes average of the space environmental monitor which is installed on GMS.

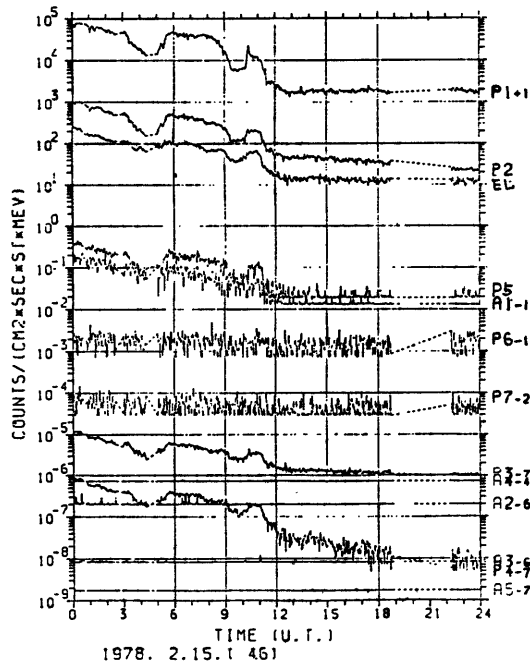
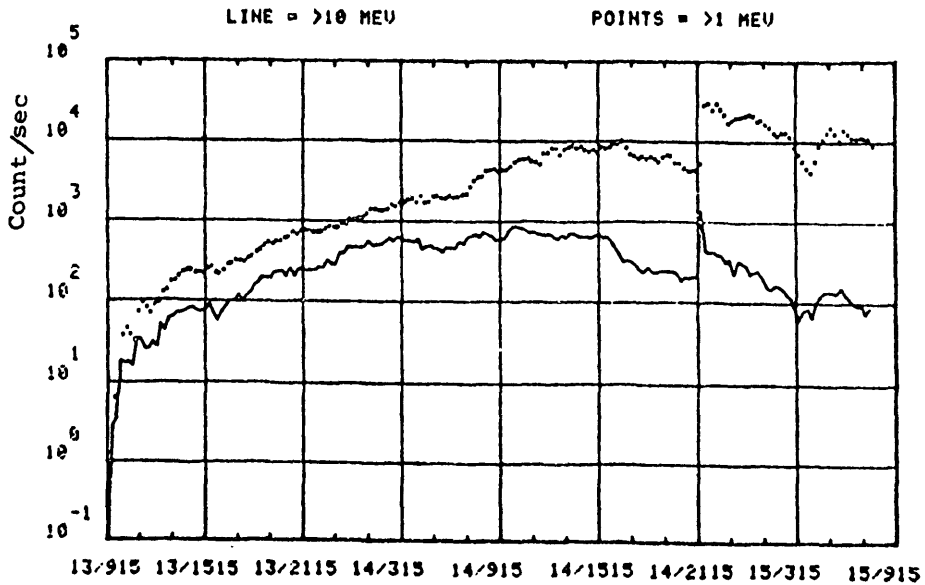


Fig. 18 The two minutes average of the space environmental monitor which is installed on GMS.



Note: At 2135U.T. 14 Feb. 1978, A geomagnetic storm began with a sudden commencement. The storm was quite intense and on 15 Feb. the auroral electrojet was flowing just north of Boulder (40 degree north latitude). The storm subsided by approximately 1400U.T., 15 Feb. (Boulder Geomagnetic Substorm Log)

Fig. 19 Proton flux plot for SMS-2 starting at 13/915.

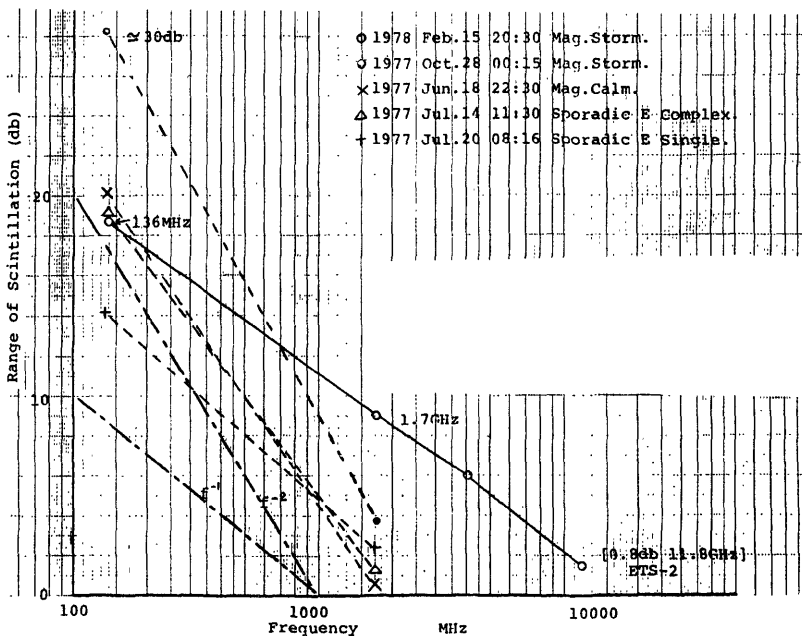


Fig. 20 Observed relations between the frequencies and the amplitude of scintillation. (K. Shinno, 1978 : Radio Regulation Laboratory of Japan)

REFERENCES

- AARONS, J. and WHITNEY, H. E. 1968: Ionospheric scintillations at 136 MHz for a synchronous satellite, *Planet. Sp. Sci.*, **16**, 21-28.
- AARNS, J., WHITNEY, H. E. and ALLEN, R. S. 1971: Global morphology of ionospheric scintillations. *Proc. IEEE*, **59**, 159-172.
- Balsley, B. B. Haerendel, G. and Gfeenwald, R. A. 1972: Equatorial spread F: Recent observations and a new interpretation, *J. Geophys. Res.*, **77**, 5625-5628.
- Chandra H. and Rastogi, R. G. 1974: Scintillations of satellite signals near the magnetic equator, *Current Science*, **43**, pp. 567-568.
- Garret H. B. -et al., 1977: Rapid Variations in Spacecraft Potential AFGL-TR-77-0132 p. 12.
- KOSTER, J. R. 1966: Ionospheric studies using the tracking beacon of the Early Bird synchronous satellite. *Aun. de geophys.*, **22**, 435-439.
- MULLEN, J. P. 1973: Sensitivity of equatorial scintillation to magnetic activity. *J. Atmos. Terr. Phys.*, **35**, 1187-1194.
- SKINNER, N. J., KELLEHER, R. F., HACKING, J. B. and BENSON, C. W. 1971: Scintillation fading of signals in the SHF band. *Nature (Physical Science)*, **23**, 19-21.
- TAUR, R. R. 1973: Ionospheric scintillations at 4 and 6 GHz. *COMSAT Technical Review*, **3**, (1).
- TAUR, R. 1974: Ionospheric scintillation at frequencies above 1 GHz. *COMSAT Technical Review*, **4**, 461-476.
- Wright et al., 1956: Spead F layer Echoes and Radiostar Scintillation, *Journal of Atmospheric and Terrestrial Physics*, **8**, 240-246.

電離層シンチレーションが GMS 回線に及ぼす影響

福井 徹郎

気象衛星センター 施設管理課

松尾 正利

気象衛星センター 気象衛星通信所

衛星通信が盛んになるにつれて、電離圏のシンチレーションが、回線に及ぼす影響が、注目されるようになってきた。本論文では、まず現在までに研究されている、シンチレーションの発生原因および観測された現象について紹介する。また、GMS 打上げ後、衛星との回線の状態は、テレメトリチャンネルを常時モニターすることにより監視しているが数多くのシンチレーションが観測されているので、その発生状況を報告し、とくに、1978年2月15日の最大級のシンチレーションについては、関連するデータも合わせて、その特徴を述べる。